Received: 13 January 2021 | Revised: 7 April 2021 | Accepted: 24 April 2021

DOI: 10.1111/vsu.13657

ORIGINAL ARTICLE - RESEARCH

WILEY

Biomechanical effects of a titanium intervertebral cage as a stand-alone device, and in combination with locking plates in the canine caudal cervical spine

Rick Beishuizen DVM[1] | Tjarda E. Reints Bok DVM[1] | Michelle Teunissen DVM[1] | Albert J. van der Veen MEng, PhD[2] | Kaj S. Emanuel MSc[2,3] | Marianna A. Tryfonidou DVM, PhD, DECVS[1] | Bjorn P. Meij DVM, PhD, DECVS[1]

[1]Department of Clinical Sciences, Faculty of Veterinary Medicine, Utrecht University, Utrecht, The Netherlands

[2]Department of Orthopedic Surgery, Amsterdam UMC, Amsterdam Movement Sciences, Amsterdam, The Netherlands

[3]Department of Orthopedic Surgery, Maastricht UMC+, Maastricht, The Netherlands

Correspondence
Rick Beishuizen, Department of Clinical Sciences, Faculty of Veterinary Medicine, Utrecht University Yalelaan 108 3584 CM Utrecht The Netherlands.
Email: rickbeishuizen@gmail.com

Funding information
Dutch Arthritis Society, Grant/Award Number: LLP22

Abstract

Objective: To evaluate the change in ex vivo biomechanical properties of the canine cervical spine, due to an intervertebral cage, both as a stand-alone device and in combination with plates.

Study Design: Experimental ex vivo study.

Animals: Cervical spinal segments (C5-C7) from eight canine cadavers.

Methods: The range of motion (ROM) and elastic zone stiffness (EZS) of the spines were determined with a four-point bending device in flexion/extension, lateral bending, and axial rotation for four conditions: native, discectomy, cage (at C6-C7), and cage with plates (at C6-C7). The disc height index (DHI) for each condition was determined using radiography.

Results: Discectomy resulted in overall increased ROM ($p < .01$) and EZS ($p < .05$) and decreased DHI ($p < .005$) when compared to the native condition. Placement of the cage increased DHI ($p < .001$) and restored total ROM during flexion/extension, lateral bending and axial rotation, and EZS during flexion/extension to the level of the native spine. Application of the plates further reduced the total ROM during flexion/extension ($p < .001$) and lateral bending ($p < .001$), but restored ROM in extension and EZS during lateral bending. No implant failure, subsidence, or significant cage migration occurred during loading.

Conclusion: An anchorless intervertebral cage used as a stand-alone device was able to restore the disc height and spinal stability to the level of the native cervical spine, whereas the addition of plates further reduced the spinal unit mobility.

This study was presented at the 28th European College of Veterinary Surgeons annual scientific meeting; July 2, 2020; Online Resident Forum.

Clinical Significance: This study implies that the intervertebral cage may be used as a stand-alone device in the spinal unit fixation in the canine cervical spine.

1 | INTRODUCTION

Canine caudal cervical spondylomyelopathy (CCSM) is a spinal disease predominantly affecting large- and giant-breed dogs.[1,2] Pathophysiology involves static and dynamic factors that result in intervertebral disc (IVD) degeneration, protrusion, vertebral canal stenosis, and vertebral foramen stenosis.[2-4] The caudal cervical spine is less rigid compared to the cranial cervical spine and the most common affected IVD is C6-C7, followed by C5-C6.[5-8] Extension of the cervical vertebral column reduces the vertebral canal and foramen diameters, adding dynamic impingement to the compression.[9,10]

Conservative management results in clinical improvement in 38%–54% of cases.[11-13] In comparison, numerous surgical techniques addressing CCSM result in 70%–90% improvement.[12,14] Surgery comprises a direct decompressive technique, for example, dorsal laminectomy or ventral slot,[14-16] or distraction-stabilization techniques, addressing the dynamic component of CCSM.[2,4,17-33]

Cervical stenotic myelopathy is the human analog disease for CCSM in dogs. Implantation of an interbody cage with or without anterior plating to attain spinal fusion is currently one of the standard surgical treatment options for cervical myelopathy in humans.[34] The stand-alone cage appears to have better clinical outcomes than the instrumented cage, despite increased rates of subsidence and less restoration of cervical lordosis.[35] Biomechanically the stand-alone cage resulted in a reduction in the range of motion (ROM). Additional plates augmented the stability of the cage but also increased rigidity, possibly explaining the better outcome of the stand-alone cage.[36] Studies have shown that the canine and human spine have similar motion patterns.[37]

Interbody cages aim to restore disc height and foraminal width and stabilize the spinal segment until bony fusion is completed. A presumed risk of the stand-alone cage is subsidence.[30] Therefore ventral vertebral body plating has been applied in the past, but increases surgical time and risk of complications such as fractures, or penetration of the vertebral canal or adjacent IVDs. These result in adjacent segment pathology (ASP) in 78% of cases and adjacent segment disease (ASD) in 11%–30% of cases.[2,14,24,29,30,33,38] The use of an anchorless cage as a stand-alone device has been reported in two dogs with CCSM, without complications. Both dogs improved neurologically, and radiographs showed osseous fusion of the affected spinal segments without cage displacement.[17,29]

The biomechanical effects of a stand-alone cage without additional anchoring in dogs have not been investigated. The objective of this study is to determine the biomechanical properties of a stand-alone anchorless intervertebral titanium cage in cadaveric canine cervical spines and to compare these to the combination of an intervertebral titanium cage with ventral locking plates. If the cage is able to restore the disc height and stabilize the spine, additional plating may not be required, reducing surgical time and complications associated to screw placement.

2 | MATERIALS AND METHODS

2.1 | Specimens

Spinal segments (C4-T1) were collected from dogs without degenerative disc disease ($n = 8$, weight: 18–58 kg,

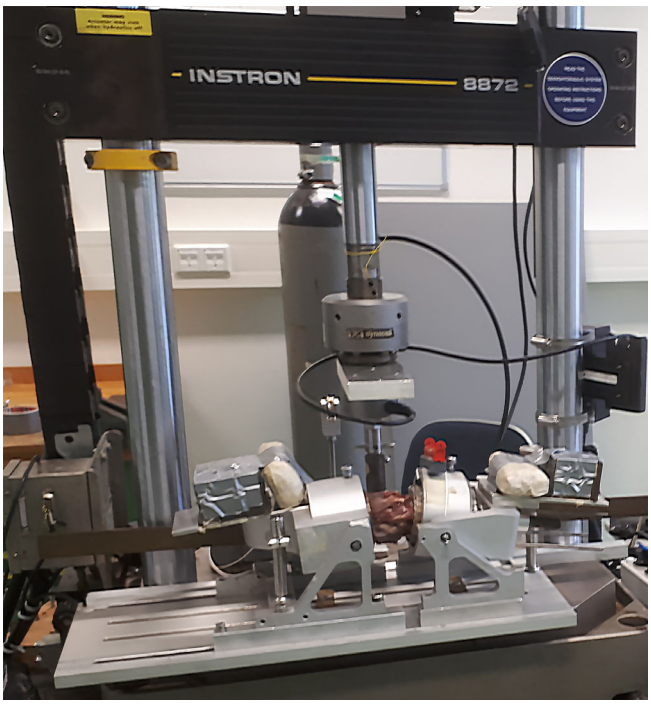

FIGURE 1 The experimental setup. The cervical segment is fixated on the cranial (C4-C5) and caudal (C7-T1) side in metal cups with the aid of screws and metal alloy. The metal cups are placed in the four-point bending and the segment of C5-C7 is loaded using a hydraulic materials-testing machine (Instron Model 8872, Instron Corporation IST, Norwood, Massachusetts)

age: 1.6–7.5 years) that were euthanized for unrelated experiments, approved by national authorities on Animal Experimentation ($n = 6$; mixed breed, AVD115002016531 and AVD1080020173964), or donated after death by the owners for research purposes ($n = 2$; Rottweiler and English fox hound).

2.2 | Specimen preparation and testing

Spinal segments were stored at −20°C in air and fluid-tight packaging material. The specimens were thawed to 4°C in a period of up to 72 h after which the segment C4-T1 was isolated from the rest of the spine. Directly after thawing, the specimens were prepared for testing and all tests were performed sequentially at 20°C. Testing cycles in between the different surgical procedures were performed in one session that lasted around 3 h from start to end for each spinal specimen. Soft tissues surrounding C4 and T1 were completely removed. Soft tissues unrelated to the biomechanical stability were removed from the C5-C7 segment, leaving axial spinal muscles (m. spinalis et semispinalis cervicis, m. multifidus cervicis, m. intertransversari cervicis, and *M. longus* colli), joint capsules, and ligaments intact.

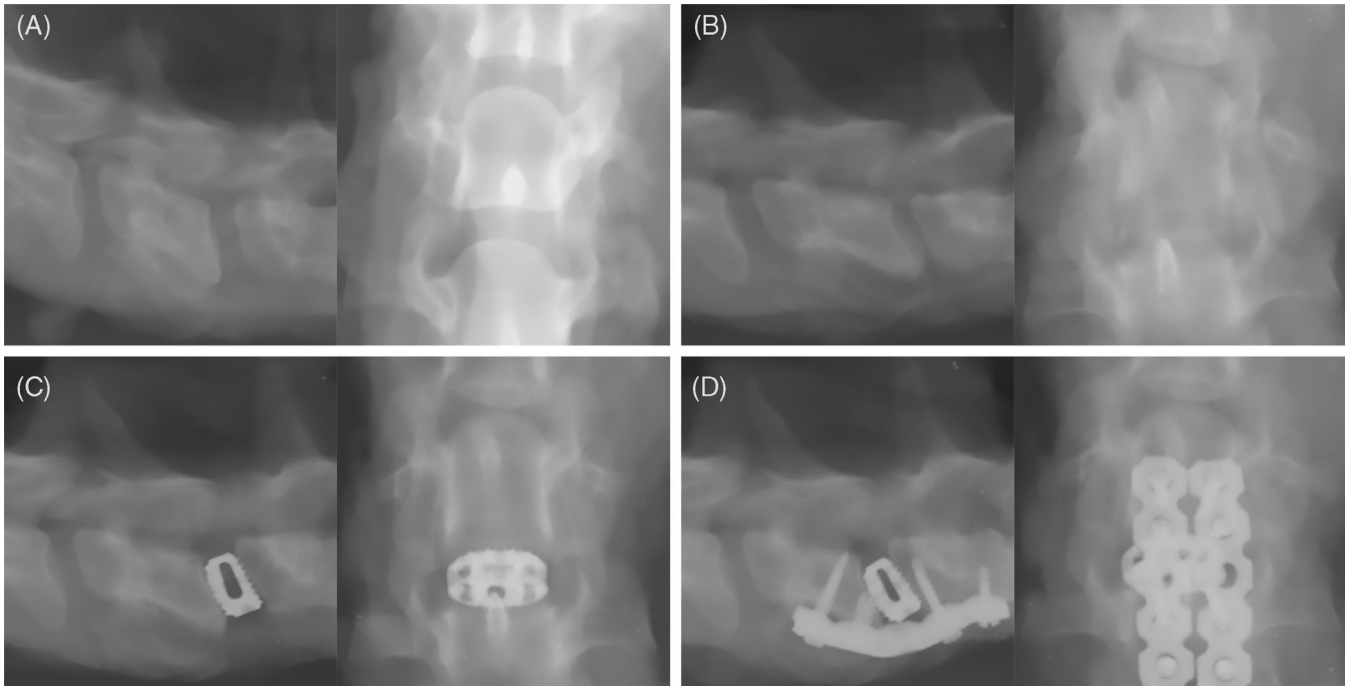

FIGURE 2 Representative lateral and dorsoventral radiographs of the C5-C7 spinal segment of one dog for the four sequential spinal conditions: native spine (A), partial ventral discectomy of C6-C7 (B), stand-alone cage inserted into C6-C7 (C), and cage in combination with plates (D)

TABLE 1 Disc height (DH) and disc height index (DHI) for every individual spine (1–8) for each of the tested conditions (native, discectomy, cage, and cage with plates)

	Native		Discectomy		Cage		Cage + plates	
Spine	DH (mm)	DHI	DH (mm)	DHI	DH (mm)	DHI	DH (mm)	DHI
1	5.28	0.23	4.13	0.19	8.79	0.37	9.24	0.38
2	5.1	0.21	3.86	0.16	7.62	0.31	7.43	0.32
3	5.51	0.26	4.87	0.22	7.82	0.37	7.66	0.37
4	5.14	0.24	4.07	0.18	7.66	0.36	8.01	0.37
5	7.73	0.25	6.52	0.22	8.11	0.28	7.75	0.26
6	5.34	0.2	4.55	0.17	7.71	0.31	7.56	0.31
7	5.78	0.24	3.96	0.16	8	0.34	8.39	0.35
8	6.34	0.25	4.48	0.17	7.71	0.34	8.17	0.35

Abbreviation: mm, millimeters.

Screws were inserted through the cranial and caudal endplate and the vertebral body of C4, through the cranial endplate of C5, into the cranial third of the length of the vertebral body of C5, effectively fusing the C4-C5 IVD space and providing holding power for fixation of the specimen. Caudally, screws were inserted through the caudal and cranial endplate and the vertebral body of T1, through the caudal endplate of C7, into the caudal third of the length of the vertebral body of C7, effectively fusing the C7-T1 IVD space and providing holding power for fixation of the specimen. The partially embedded screws and vertebral bodies of C4 and T1 were fixed in a neutral position in metal cups, which were then filled with a heated alloy (Cerro-low147; Cerro Metal Products Company, Bellefonte, Pennsylvania). The segments were kept moist by regular spraying with saline (0.9% NaCl), were placed in a four-point bending device with the neutral axis of the spine aligned to the central axis of the fixtures,[39] and were loaded using a hydraulic materials-testing machine (Instron Model 8872, Instron Corporation IST, Norwood, Massachusetts) (Figure 1). The loading protocol was displacement-driven. The angular displacement was applied by the system with a velocity of 0.5°/s until a maximum bending or rotation moment of 1 Nm was reached. The necessary moment was determined by multiplying the moment arm of the system with the force, measured by a force transducer. A cyclic moment from +1 to −1 Nm was repeated 10 times. The ROM was defined as the difference in angles at 1 and −1 Nm.

Spinal segments were tested at the level of C5-C7 in flexion/extension, lateral bending, and axial rotation for each of the following conditions: native spine, discectomy, stand-alone cage, and cage in combination with plates. The native unmodified spine was tested first to acquire baseline values. Next, discectomy of C6-C7 was performed. A rectangular window (10 × 5 mm) was removed from the ventral annulus fibrosus, followed by complete removal of the nucleus pulposus. The spinal segment C6-C7 was distracted manually by forcing the metal cups in opposite directions, thus opening the IVD space. The cartilaginous layers of the endplates were removed using a curette, carefully preserving the cortical bone of the endplates. Using an implant holder (396.891, DePuy Synthes, Johnson-Johnson, Switzerland), a trial cage (Curved trial implant, 396.610, DePuy Synthes) was inserted to determine if the final implant would fit accurately in the IVD space. The trial cage was removed and the titanium cage (SynCage-C short implant, curved, 495.221S, DePuy Synthes) was inserted in the C6-C7 disc space. The cage dimensions were 15 × 12.5 × 4.5 mm. The cranial surface of de cage was concave and the caudal surface flat. Both surfaces contained a central opening (measuring 5 mm in diameter) and seven surrounding smaller openings (measuring 2 mm in

TABLE 2 Range of motion (ROM) and elastic zone stiffness (EZS) during flexion/extension, lateral bending, and axial rotation, for each of the tested conditions (native, discectomy, cage, and cage with plates)

	Flexion/extension				Lateral bending				Axial rotation			
	Native	Discectomy	Cage	Cage + plates	Native	Discectomy	Cage	Cage + plates	Native	Discectomy	Cage	Cage + plates
Total ROM[a]	24.7 ± 5.6	31.15 ± 6.4	24.05 ± 5.63	15.93 ± 4.29	36.8 ± 7.2	41.9 ± 3.4	34 ± 4.3	24.8 ± 5.5	8.1 ± 3.8	18 ± 5	6.1 ± 3.2	5.7 ± 2.7
ROM[a] during extension	12.6 ± 2.95	16 ± 3	15.8 ± 2.9	10.1 ± 3.5								
ROM[a] during flexion	12.2 ± 3.5	15.2 ± 3.9	8.2 ± 3.3	5.8 ± 1.5								
EZS[b]	0.30 ± 0.05	0.39 ± 0.1	0.26 ± 0,07	0.35 ± 0.09	0.33 ± 0.04	0.44 ± 0.06	0.26 ± 0.04	0.3 ± 0.05	0.25 ± 0.16	0.18 ± 0.06	0.33 ± 0.2	0.41 ± 0.42

[a]ROM displayed as the median angular displacement, in ° with the interquartile range.
[b]EZS displayed as the median stiffness, in Nm/° with the interquartile range.

diameter) that allow bony ingrowth through the cage. The lateral sides of the cage contain a single opening measuring 7.2 × 2.5 mm. The cranial and caudal surfaces and both sides of the cage contain 51 spikes, measuring 1 × 1.2 mm, to provide an optimal implant–endplate interface, limiting the risk of migration. Lastly, the spine was stabilized using two parallel five-hole titanium locking 2.4 mm plates (UniLOCK reconstruction plate 2.4, 449.612, DePuy Synthes) with 2.4 mm self-tapping locking titanium screws (UniLOCK screw 2.4 self-tapping, 497.67X, DePuy Synthes), as described by Voss et al.[27] The plates were adapted to the ventral surface of C6 and C7 and fixated with two screws in C6 and two screws in C7, for each plate, leaving the screw hole crossing the C6-C7 disc space empty.

2.3 | Imaging

Ventrodorsal and lateral radiographs were taken of the native spine, after partial discectomy, after insertion of the cage, and after application of plating (Figure 2). The radiographs were examined using a RadiAnt DICOM Viewer (version 2.2.3, Medixant, Poland). The disc height was measured at the center of the disc on lateral radiographs and the disc height index (DHI) was calculated based on the lateral radiographs using the method described by Willems et al. (Table 1).[40]

2.4 | Data analysis

The total ROM in flexion/extension, lateral bending and axial rotation, and the elastic zone stiffness (EZS) were determined for the four conditions of each cervical spinal segment (Table 2), by joining the loading cycles and using the average angular displacement or average stiffness for further analysis (Figure 3). Additionally, the ROM in flexion and extension were calculated separately, because head carriage might influence these factors differently. The ROM in lateral bending to the right or left and the ROM in axial rotation to the right or left were not calculated separately, because any differences would likely be attributable to slight asymmetrical placement of the specimens in the cups or because of asymmetry in the spines themselves. The total ROM was defined as the angular displacement between the minimum (−1 Nm) and the maximum (+1 Nm) loads. The EZS was defined as the slope of the linear fit over the final degree of motion that is approaching the maximum of the range, in Nm/degree. The maximum of the range was reached during flexion, lateral bending to the right, and axial rotation to the left. Near the maximum, the angular deformation characterizes the elastic deformation of the specimen.[41] Displacement and force were measured at 100 Hz. Analysis was conducted using

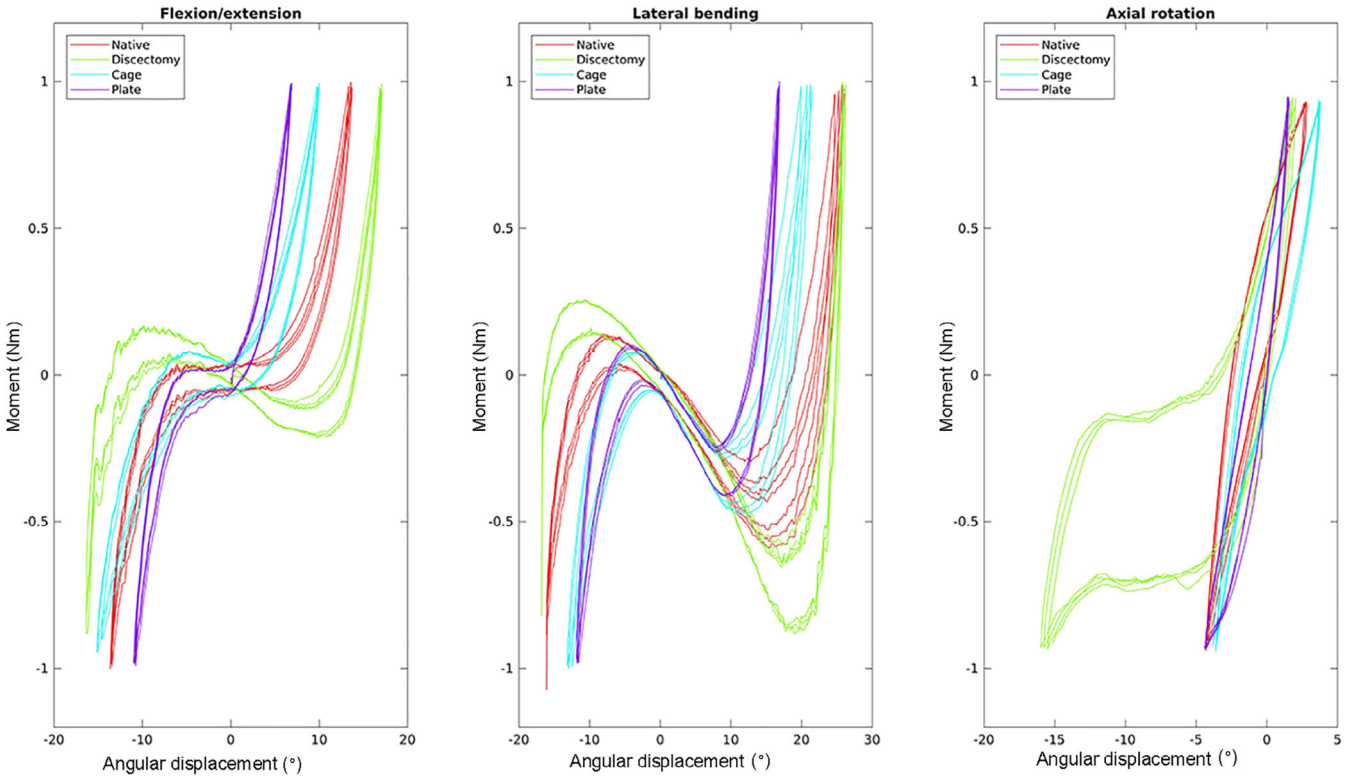

FIGURE 3 Representative load–displacement curves of the spinal segment of Dog 7, in the four tested conditions (native, discectomy, cage, and cage with plates), for flexion/extension, lateral bending, and axial rotation

in-house developed scripts in MATLAB R2018A (Mathworks, Natwick, Massachusetts).

2.5 | Statistics

Statistical analysis was performed using R statistical software version 3.0.2. A linear mixed model, containing both fixed and random effects, was used to analyze DHI, ROM, and EZS. The four conditions of each spine and the interaction between these conditions were taken as a fixed effect. The canine donor was considered as a random effect. Based on the Akaike Information Criterion, an optimal model was chosen. A QQ plot and Shapiro–Wilk normality test of the residuals were used to assess normal distribution of the data. A Benjamini–Hochberg correction was used to account for the multiple comparisons. A p-value of <.05 was considered significant. Additionally the corresponding Cohen's d effect size (ES) and CI were calculated (Appendix S1).

3 | RESULTS

Radiographs of each spine did not show evidence of anomalies, degenerative disc disease, discospondylitis, or zygapophyseal joint arthrosis, nor was there loss in the DHI of the treated segment compared to the adjacent levels. Macroscopic evaluation showed that after discectomy only the ventral annulus fibrosus and nucleus pulposus were removed, as intended, and no signs of degenerative disc disease or discospondylitis were present. Cage insertion was possible in all eight spines after careful curettage of the endplates and slight manual distraction of the spinal segment. None of the endplates were perforated after curettage. During testing of the spines, no cage failure, subsidence, or cage migration was noticed in seven of the eight spines. In one spine, the cage migrated 1 mm ventrally after the first bending sequence and then remained in the same position during the remainder of the test. After contouring the plates, all screws were properly inserted with sufficient bone engagement, as determined by radiography. During testing, no implant failure, implant loosening, or implant migration occurred. After data analysis, 37 parameters showed a significant p-value prior to Benjamini–Hochberg correction. After correction, 35 p-values remained significant, revealing two false discoveries.

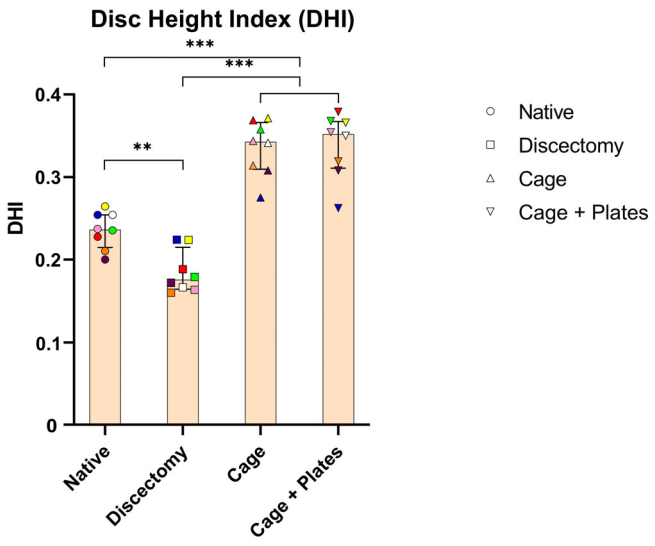

FIGURE 4 Disc height index (DHI) displayed as the median DHI for the four spinal conditions (native, discectomy, cage, and cage with plates) with the interquartile and total ranges. Each different color depicts an individual spine. **p < .01; ***p < .001

The DHI of the C6-C7 IVD decreased after discectomy (ES −2.24, p = .001). Cage placement resulted in an increase of the DHI compared to discectomy (ES 5.38, p < .001), and the native spine (ES 3.74, p < .001). Plate fixation did not result in a further increase of the DHI (p = .814) (Figure 4).

The total ROM during flexion/extension increased after discectomy (ES 1.14, p = .001). After placement of the cage, the total ROM during flexion/extension decreased (ES 1.26, p < .001), reaching a total ROM comparable to the total ROM in the native condition (p = .687). After application of the plates, the total ROM during flexion/extension decreased versus the native spine (ES −1.88, p < .001), the spine after discectomy (ES −2.99, p < .001), and the spine after cage placement (ES −1.73, p < .001) (Figure 5(A)). Both ROM in flexion (ES 0.87, p = .006) and ROM in extension (ES 1.23, p = .007) increased after discectomy. After cage placement, the ROM in flexion decreased (ES −2.05, p < .001) and the ROM in extension remained unchanged (p = .765). Compared to the native spine, ROM in flexion was decreased after cage placement (ES −1.24, p < .001), and ROM in extension was increased after cage placement (ES 1.18, p = .008). Application of the plates resulted in a further reduction of the ROM in flexion (ES −1.01, p = .012) and a reduction of the ROM in extension (ES −1.89, p < .001). The ROM in flexion was decreased versus the native spine (ES −2.51, p < .001) and the spine after discectomy (ES −3.37, p < .001). The ROM in extension was comparable to the native spine (ES −0.82, p = .053) but decreased compared to the spine after discectomy (ES −1.93, p < .001) (Figure 5(A)).

The total ROM during lateral bending increased after discectomy (ES 0.99, p = .003). Cage placement resulted in a decrease in lateral bending versus the spine after discectomy (ES −2.22, p < .001), but was comparable to the native spine (ES −0.5, p = .087). Plate fixation decreased

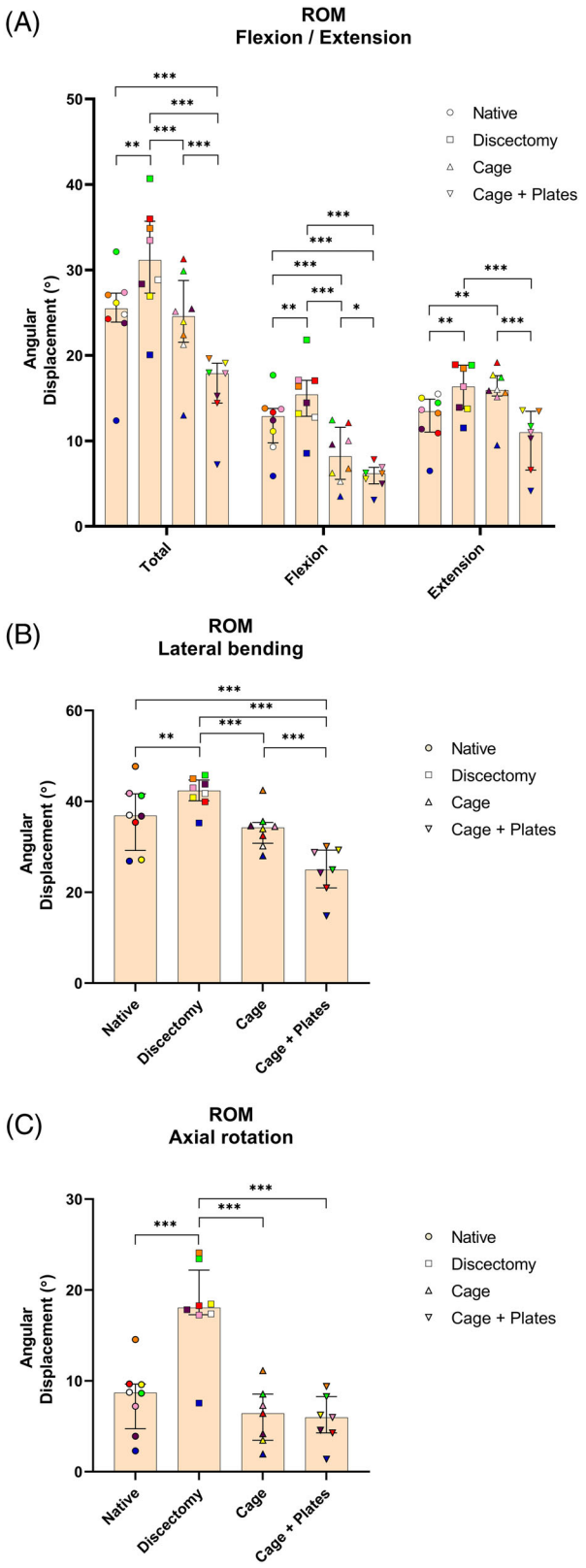

FIGURE 5 Range of motion (ROM) during flexion/extension (A), lateral bending (B), and axial rotation (C), displayed as the median angular displacement (°) with the interquartile and total ranges for each of the tested conditions (native, discectomy, cage, and cage with plates). *$p < .05$; **$p < .01$; ***$p < .001$

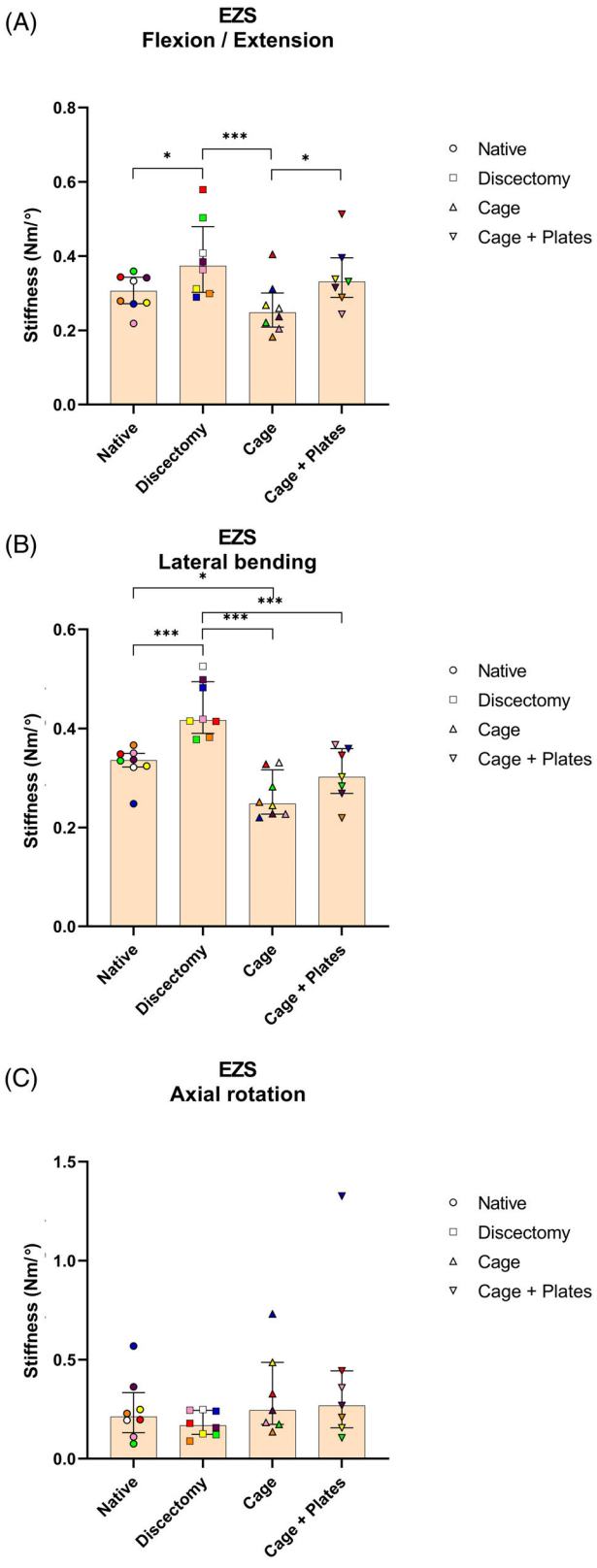

FIGURE 6 Elastic zone stiffness (EZS) during flexion/extension (A), lateral bending (B), and axial rotation (C), displayed as the median stiffness (Nm/°) with the interquartile and total ranges for each of the tested conditions (native, discectomy, cage, and cage with plates). *$p < .05$; **$p < .01$; ***$p < .001$

the total ROM during lateral bending versus the native spine (ES −2.02, $p < .001$), the spine after discectomy (ES −4.05, $p < .001$), and the spine after cage placement (ES −2.02, $p < .001$) (Figure 5(B)).

In axial rotation, the total ROM increased after discectomy (ES 2.4, $p < .001$) and decreased after cage placement (ES −3.02, $p < .001$). Plate fixation did not result in a further decrease ($p = .742$). The total ROM in axial rotation did not differ between the native spine and the spine after cage placement ($p = .153$), or after plate fixation ($p = .101$) (Figure 5(C)).

During flexion/extension, the EZS increased after discectomy (ES 4.81, $p = .015$) and decreased after cage placement (ES −1.59, $p = .001$), resulting in a EZS similar to the native spine ($p = .175$). Additional plate fixation increased the EZS (ES 1.15, $p = .020$) versus the spine after cage placement, while there was no difference compared to the native spine ($p = .175$) or the spine after discectomy ($p = .175$) (Figure 6(A)). During lateral bending, EZS increased after discectomy (ES 2.53, $p < .001$) and decreased after cage placement (ES −3.72, $p < .001$), resulting in a EZS smaller versus the native spine (ES −1.71, $p = .020$). Additional plate fixation did not change the EZS compared to the spine after cage placement ($p = .121$), while it was similar to the EZS of the native spine ($p = .380$) and was smaller compared to the EZS of the spine after discectomy (ES −2.59, $p < .001$) (Figure 6(B)). During axial rotation, no significant changes were found between EZS of the different spine conditions (Figure 6(C)).

4 | DISCUSSION

After discectomy, the stand-alone anchorless intervertebral cage was able to increase the DHI and to restore spinal stability and motion up to a level comparable to the native condition. Additional ventral locking plate fixation resulted in a further decrease of total spinal ROM in lateral bending and flexion and extension beyond the native spine stability. Plates restored ROM in extension and EZS in lateral bending to the native condition.

Compared to the human biomechanical studies[36,42] evaluating the stand-alone interbody cage, our study revealed similar results. The stand-alone cage resulted in a significant reduction in the ROM in all directions. Additional plates resulted in a further reduction, augmenting the stability of the cage but also increasing spinal rigidity. A canine study evaluating the biomechanical effects of an intervertebral fusion cage with integrated ventral fixation and fixation with a ventral locking plate also revealed similar results. Both the anchored cage and locking plate fixation resulted in a decrease in ROM; however, there were no significant differences between the two techniques.[20]

Extension of the cervical spine decreases the dimensions of the already stenotic vertebral foramen and vertebral canal in dogs with CCSM[10] and causes pain. Discectomy results in a significant increase in the ROM in extension, which might exacerbate compression during extension, which is a hallmark of the dynamic compression seen in CCSM. Although cage placement does not reduce the ROM in extension, dynamic compression is most likely decreased or absent due to an increased disc height and removal or stretching of the dorsal annular protruding tissue. Additional plating does restore ROM in extension to the native condition. Apparently plate-induced spinal rigidity simulates the ligamentous stability of the normal spine. Therefore, additional plating should be considered if the amount of DHI increase, related to the cage fit and stability, is deemed inadequate to relieve dynamic compression during extension.

Although discectomy results in decreased rigidity of the spine, and the cage in increased rigidity, the EZS during flexion/extension and lateral bending increases after discectomy and decreases after cage placement. The unexpected increased EZS during flexion/extension and lateral bending after discectomy might be explained by the fact that the annulus fibrosus will no longer gradually tension after discectomy. The zygapophyseal joints and ligaments will eventually tension, but apparently with much more rigidity than the annulus fibrosis.

Fusion or stabilization of one IVD space increases the pressure and ROM at the adjacent disc spaces up to 24%.[14,38] These increased stresses may lead to adjacent disc protrusion, or hypertrophy of annular or ligamentous structures, the so-called ASP.[11] The stand-alone cage allows for more flexion and extension than the cage combined with the plates. A non-instrumented stand-alone cage possible reduces the stress on adjacent segments and therefore the chance of ASP. However, bony fusion through the cage will occur eventually, possibly eliminating this difference.[29] ASP can also be caused by progressive spontaneous degeneration of IVDs over time or the negative effects of the spinal implants (screws, plates) on the IVDs or endplate.[43] The main biomechanical force leading to IVD degeneration in dogs, and thereby a possible contributing factor to ASP after vertebral fixation/fusion, is axial rotation.[7,8] While discectomy resulted in an increased total ROM during axial rotation, cage placement normalized total ROM in axial rotation. Additional plate fixation did not result in a further decrease of total ROM in axial rotation and is therefore not advantageous over a stand-alone cage to prevent development of ASP as a result of the axial rotation.

Although cage displacement is a presumed risk without plating, only one of eight cages showed minor ventral displacement after the first run and remained in the same

position for the rest of the test. The displacement did not progress and did not require intervention. The shape of the cage, the size of the footplate, the perforations, and spikes are designed to provide an optimal implant–endplate interface, limiting the risk of migration. Displacement ex vivo might occur more easily because surrounding soft-tissue structures and muscle tension were lacking in the cadaveric spine specimens. Long-term in vivo studies in dogs with CCSM treated with stand-alone cages are necessary to evaluate the viability of this technique.

Other risks of the stand-alone cage include non-union of the spinal segment and subsidence of the cage. Although no subsidence was or could be noted in this biomechanical study, long-term in vivo studies are necessary to evaluate the true occurrence of subsidence and also the risk of non-union. Two previous studies reported on two dogs with CCSM that were treated successfully with an anchorless stand-alone cage. Long-term follow-up described bony fusion without complications such as cage displacement or subsidence.[17,29] A recent study investigating the short-term clinical and radiographical outcome after application of an anchored intervertebral spacer in 37 dogs with disc-associated cervical spondylomyelopathy showed subsidence of the anchored cage in 40% and screw loosening and/or breakage in 59%.[19] This may be caused by difference in design of the cage (smaller footplate acting as a stress riser) and the use of 2.0 mm screws. The high incidence of screw loosening was taken into consideration and modification of the implant with a new locking system and new screw dimensions was required; however, the footplate design remained unchanged.[19]

The present study has several limitations. Inherent to the ex vivo nature of this study, statistical differences cannot be directly extrapolated to clinical significant changes. However, the magnitude of change (illustrated by the ES) can make clinical significance more likely. Although ligaments, joint capsules, and axial muscles remained in place, the biomechanical testing did not include the possible stabilizing effect of other surrounding musculature or the incorporation of bone graft through the cage, which would have been applied in vivo. Another limitation is posed by the effect of adjacent fixated (C4-C5 and C7-T1) and free-moving (C5-C7) segments on the segment of interest (C6-C7). Fixated segments might cause the construct to appear more rigid whereas free-moving segments could cause the construct to appear less rigid. These effects do not change the direction of changes measured, but could have an effect on the amount of change. This study was also limited by the individual differences between spinal specimens, originating from dogs that ranged both in body weight and age. Size and bone mineral density can vary between specimens and might have an effect on stability, cage fit and bone engagement. Another limitation is the relative small number of loading cycles. Although no significant cage migration or subsidence was noted, it might still occur after a larger number of cycles.

In conclusion, the anchorless intervertebral titanium cage used as a stand-alone device restored the DHI, total ROM during flexion/extension, lateral bending and axial rotation and EZC during flexion/extension to the level of stiffness of the native spine. Additional ventral plating resulted in an additional restoration of EZS during lateral bending and ROM in extension, but also caused a decreased total ROM during flexion/extension and lateral bending. It is conceivable that this added spinal rigidity might increase the chance of ASP. Therefore, the intervertebral cage used as a stand-alone device may provide a good alternative to the instrumented cage, since it restores spinal stability without adding spinal rigidity, while restoring disc height. From a clinical perspective, sufficient coverage of the cage footplate over the endplate seems to be essential to decrease the stress risers on the endplate, which may otherwise increase the risk for subsidence. It remains to be elucidated whether the additional restoration of EZS during lateral bending and ROM in extension outweighs the loss of spinal mobility when ventral plates are added, especially since the stand-alone cage provides adequate stability and restoration of DHI, without significant risk of ventral cage displacement. Although the anchorless stand-alone device has successfully and safely been used in vivo in a limited number of clinical cases, more research is necessary regarding the in vivo biomechanical consequences in the long term, the risk of cage migration, non-union and subsidence in the long term, and the biomechanical effects of bony ingrowth through the cage.

ACKNOWLEDGMENTS

All authors contributed to the study design, collection and interpretation of data, and writing of the manuscript. The titanium intervertebral cages were donated by DePuy Synthes. The UniLOCK plates and screws were bought at commercial prices from DePuy Synthes in the Netherlands. MAT and BPM are being supported by the Dutch Arthritis Society (LLP22).

CONFLICT OF INTEREST

The titanium intervertebral cages were donated by DePuy Synthes. The UniLOCK plates and screws were bought at commercial prices from DePuy Synthes in the Netherlands. MAT and BPM are being supported by the Dutch Arthritis Society (LLP22). Funders had no influence on the study design, data analysis and data interpretation. The authors report no financial or other conflicts related to this study.

REFERENCES

1. Breit S, Künzel W. Osteological features in pure-bred dogs predisposing to cervical spinal cord compression. *J Anat*. 2001; 199(5):527-537.
2. da Costa RC. Cervical spondylomyelopathy (wobbler syndrome) in dogs. *Vet Clin North Am – Small Anim Pract*. 2010; 40(5):881-913.
3. Burbidge HM, Pfeiffer DU, Blair HT. Canine wobbler syndrome: a study of the dobermann pinscher in New Zealand. *N Z Vet J*. 1994;42(6):221-228.
4. Denny HR, Gibbs C, Gaskell CJ. Cervical spondylopathy in the dog—a review of thirty-five cases. *J Small Anim Pract*. 1977;18 (2):117-132.
5. da Costa RC, Echandi RL, Beauchamp D. Computed tomography myelographic findings in dogs with cervical spondylomyelopathy. *Vet Radiol Ultrasound*. 2012;53(1):64-70.
6. da Costa RC. Relationship between spinal cord signal changes and clinical and MRI findings in dogs with cervical spondylomyelopathy: 102 cases. *J Vet Intern Med*. 2012;26:807.
7. Farfan HF, Cossette JW, Robertson GH, Wells RV, Kraus H. The effects of torsion on the lumbar intervertebral joints: the role of torsion in the production of disc degeneration. *J Bone Joint Surg Am*. 1970;52(3):468-497.
8. Johnson JA, da Costa RC, Bhattacharya S, Goel V, Allen MJ. Kinematic motion patterns of the cranial and caudal canine cervical spine. *Vet Surg*. 2011;40(6):720-727.
9. White AA, Panjabi MM. Biomechanical considerations in the surgical management of cervical spondylotic myelopathy. *Spine (Phila Pa 1976)*. 1988;13(7):856-860.
10. Ramos RM, da Costa RC, Oliveira ALA, Kodigudla MK, Goel VK. Effects of flexion and extension on the diameter of the caudal cervical vertebral canal in dogs. *Vet Surg*. 2015;44 (4):459-466.
11. Sharp N, Wheeler S. Cervical spondylomelopathy. *Small Animal Spinal Disorders, Diagnosis and Surgery*; St. Louis Missouri, USA: Elsevier Mosby; 2005:211-246.
12. da Costa RC, Parent JM, Holmberg DL, Sinclair D, Monteith G. Outcome of medical and surgical treatment in dogs with cervical spondylomyelopathy: 104 cases (1988–2004). *J Am Vet Med Assoc*. 2008;233(8):1284-1290.
13. De Decker S, Bhatti SFM, Duchateau L, et al. Clinical evaluation of 51 dogs treated conservatively for disc-associated wobbler syndrome. *J Small Anim Pract*. 2009;50(3):136-142.
14. Jeffery N. The 'wobbler' syndrome. *Handbook of Small Animal Spinal Surgery*; Philadelphia, PA, USA: W B Saunders Co; 1995:169-186.
15. De Risio L, Muñana K, Murray M, Olby N, Sharp NJH, Cuddon P. Dorsal laminectomy for caudal cervical spondylomyelopathy: postoperative recovery and long-term follow-up in 20 dogs. *Vet Surg*. 2002;31(5):418-427.
16. Rossmeisl JH, Lanz OI, Inzana KD, Bergman RL. A modified lateral approach to the canine cervical spine: procedural description and clinical application in 16 dogs with lateralized compressive myelopathy or radiculopathy. *Vet Surg*. 2005;34(5): 436-444.
17. da Silva CA, Bernard F, Bardet JF. Caudal cervical arthrodesis using a distractable fusion cage in a dog. *Vet Comp Orthop Traumatol*. 2010;23(3):209-213.
18. Farrokhi MR, Torabinezhad S, Ghajar KA. Pilot study of a new acrylic cage in a dog cervical spine fusion model. *J Spinal Disord Tech*. 2010;23(4):272-277.
19. Rohner D, Kowaleski MP, Schwarz G, Forterre F. Short-term clinical and radiographical outcome after application of anchored intervertebral spacers in dogs with disc-associated cervical Spondylomyelopathy. *Vet Comp Orthop Traumatol*. 2019;32(2):158-164.
20. Schöllhorn B, Bürki A, Stahl C, Howard J, Forterre F. Comparison of the biomechanical properties of a ventral cervical intervertebral anchored fusion device with locking plate fixation applied to cadaveric canine cervical spines. *Vet Surg*. 2013;42 (7):825-831.
21. Joffe MR, Parr WCH, Tan C, Walsh WR, Brunel L. Development of a customized Interbody fusion device for treatment of canine disc-associated cervical spondylomyelopathy. *Vet Comp Orthop Traumatol*. 2019;32(1):79-86.
22. Tuan J, Solano MA, Fitzpatrick N. Ventral distraction-stabilization in 5 continuous sites for the treatment of cervical spondylomyelopathy in a great Dane. *Vet Surg*. 2019;48(4): 607-614.
23. Solano MA, Fitzpatrick N, Bertran J. Cervical distraction-stabilization using an intervertebral spacer screw and string-of pearl (SOP™) plates in 16 dogs with disc-associated wobbler syndrome. *Vet Surg*. 2015;44(5):627-641.
24. Trotter EJ. Cervical spine locking plate fixation for treatment of cervical spondylotic myelopathy in large breed dogs. *Vet Surg*. 2009;38(6):705-718.
25. Mckee WM, Butterworth SJ, Scott HW. Management of cervical spondylopathy-associated intervertebral disc protrusions using metal washers in 78 dogs. *J Small Anim Pract*. 1999;40 (10):465-472.
26. Bergman RL, Levine JM, Coates JR, Bahr A, Hettlich BF, Kerwin SC. Cervical spinal locking plate in combination with cortical ring allograft for a one level fusion in dogs with cervical spondylotic myelopathy. *Vet Surg*. 2008;37(6):530-536.
27. Voss K, Steffen J, Montavon PM. Use of the ComPact UniLock system for ventral stabilization procedures of the cervical spine: a retrospective study. *Vet Comp Orthop Traumatol*. 2006;19(1): 21-28.
28. Lincoln JD, Pettit G. D. Evaluation of fenestration for treatment of degenerative disc disease in the caudal cervical region of large dogs. *Vet Surg*. 1985;14(3):240-246.
29. Reints Bok TE, Willemsen K, Rijen MHP, Grinwis GCM, Tryfonidou MA, Meij BP. Instrumented cervical fusion in nine dogs with caudal cervical spondylomyelopathy. *Vet Surg*. 2019; 48(7):1287-1298.
30. Steffen F, Voss K, Morgan JP. Distraction-fusion for caudal cervical spondylomyelopathy using an intervertebral cage and locking plates in 14 dogs. *Vet Surg*. 2011;40(6):743-752.
31. De Decker S, Caemaert J, Tshamala MC, et al. Surgical treatment of disk-associated wobbler syndrome by a Distractable vertebral titanium cage in seven dogs. *Vet Surg*. 2011;40(5): 544-554.
32. Adamo PF, Kobayashi H, Markel M, Vanderby R. In vitro biomechanical comparison of cervical disk arthroplasty, ventral slot procedure, and smooth pins with polymethylmethacrylate fixation at treated and adjacent canine cervical motion units. *Vet Surg*. 2007;36(8):729-741.

33. Adamo PF, da Costa RC, Kroll R, Giovannella C, Podell M, Brofman P. Cervical disc arthroplasty using the Adamo Spinal Disc® in 30 dogs affected by disc associated wobbler syndrome at single and multiple levels. *J Vet Intern Med*. 2014;28:949-950.
34. Bakhsheshian J, Mehta VA, Liu JC. Current diagnosis and management of cervical spondylotic myelopathy. *Glob Spine J*. 2017;7:572-586.
35. Cheung ZB, Gidumal S, White S, et al. Comparison of anterior cervical discectomy and fusion with a stand-alone Interbody cage versus a conventional cage-plate technique: a systematic review and meta-analysis. *Glob Spine J*. 2019;9(4):446-455.
36. Tsitsopoulos PP, Voronov LI, Zindrick MR, et al. Biomechanical stability analysis of a stand-alone cage, static and rotational-dynamic plate in a two-level cervical fusion construct. *Orthop Surg*. 2017;9(3):290-295.
37. Smit TH. The use of a quadruped as an in vivo model for the study of the spine – biomechanical considerations. *Eur Spine J*. 2002;11(2):137-144.
38. Hakozaki T, Ichinohe T, Kanno N, et al. Biomechanical assessment of the effects of vertebral distraction-fusion techniques on the adjacent segment of canine cervical vertebrae. *Am J Vet Res*. 2016;77(11):1194-1199.
39. Rustenburg CME, Kingma I, Holewijn RM, et al. Biomechanical properties in motion of lumbar spines with degenerative scoliosis. *J Biomech*. 2019;102:109495.
40. Willems N, Bach FC, Plomp SGM, et al. Intradiscal application of rhBMP-7 does not induce regeneration in a canine model of spontaneous intervertebral disc degeneration. *Arthritis Res Ther*. 2015;17(1):1-14.
41. Wilke HJ, Wenger K, Claes L. Testing criteria for spinal implants: recommendations for the standardization of in vitro stability testing of spinal implants. *Eur Spine J*. 1998;7(2):148-154.
42. Shimamoto N, Cunningham BW, Dmitriev AE, Minami A, McAfee PC. Biomechanical evaluation of stand-alone interbody fusion cages in the cervical spine. *Spine (Phila Pa 1976)*. 2001;26(19):432-436.
43. Hilibrand AS, Robbins M. Adjacent segment degeneration and adjacent segment disease: the consequences of spinal fusion? *Spine J*. 2004;4(6):190-194.

SUPPORTING INFORMATION

Additional supporting information may be found online in the Supporting Information section at the end of this article.

How to cite this article: Beishuizen R, Reints Bok TE, Teunissen M, et al. Biomechanical effects of a titanium intervertebral cage as a stand-alone device, and in combination with locking plates in the canine caudal cervical spine. *Veterinary Surgery*. 2021;50(5):1087–1097. https://doi.org/10.1111/vsu.13657